Regular Article

ANALYTICAL AND BIOANALYTICAL CHEMISTRY RESEARCH

Published by the Iranian Chemical Society

Anal. Bioanal. Chem. Res., Vol. 9, No. 2, 191-200, April 2022.

The Corrosion Control of Temporary Magnesium (AZ31 alloy) Implants Using Electrospinning Polycaprolactone-curcumin Nanofiber Coatings

Saba Dabirian[a], Soheila Kashanian[a,b,c,*], Maryam Nazari[a] and Elham Arkan[c]

[a]*Faculty of Chemistry, Razi University, Kermanshah, Iran*

[b]*Nanobiotechnology Department, Faculty of Innovative Science and Technology, Razi University, Kermanshah, Iran*

[c]*Nano Drug Delivery Research Center, Faculty of Pharmacy, Kermanshah University of Medical Sciences, Kermanshah, Iran*

(Received 7 May 2021 Accepted 28 October 2021)

In this article, polycaprolactone (PCL) polymer nanofibers have been used in the presence of curcumin (Cur) to control the corrosion rate of temporary magnesium (alloy AZ31) implants. PCL, PCL-Cur, and sodium alginate (SA)-polyvinyl alcohol (PVA)/PCL-Cur polymers coating were produced. The mentioned nanofibers were produced using a simple and cost-effective electrospinning technique. We used different techniques to examine the properties of the produced fibers, and it was demonstrated that the hydrophobic produced nanofibers with a contact angle of 135.2 degrees have continuous strands and a diameter of 171.57 nm. The presence of Cur inside PCL nanofiber not only did not have any effect on the PCL nanofiber morphology, but also increased adhesion of the coating, and 74.59% of Cur was released after 7 days. To investigate the effects of different polymeric coatings on the surface of Mg metal in the simulated body fluid (SBF), SEM, weight measurement tests, pH measurement, Polarization, and Electrochemical Impedance Spectroscopy (EIS) has been used. During the study period, there was no degradation in any part of the PCL-Cur hydrophobic polymer coating. For this coating, the percentage of weight loss, pH value, corrosion potential (E_{corr}), and corrosion rate (C_R) were 0.19%, 8.39, -1.388 V, and 0.198 mm/y, respectively, where these values indicate the significant decrease in corrosion rate while using PCL-Cur coating.

Keywords: Corrosion, Electrospinning, Implants, Magnesium AZ31 alloy, Polymer coatings

INTRODUCTION

Metals and alloys have been used in the human body as biomaterials to repair, replace, or augment tissues and structures for many decades [1]. Biological materials used as implants should have the characteristics of stiffness, strength, corrosion resistance, and they should not cause more infection and inflammation to the damaged tissues, especially within the early days [2].

Implants are divided into two groups: permanent and temporary. We require the necessity of a secondary surgery to remove temporary implants, which is not cost-effective and it also may cause pain to the patient [3]. So, it would be better to use degradable metals such as Magnesium (Mg) and its alloys [3-5] in the physiological environment of the body. The significant advantages of Mg alloys over other biomaterials are as follows:

(i) Mg has elastic modulus of ~43 GPa which is close to that of bone minimizing stress shielding effect [6-10]. (ii) High strength-to-weight ratio of Mg makes it suitable for load-bearing applications [11]. (iii) Mg is essential for several metabolic processes [9,11-14]. (iv) Excessive amounts of Mg do not cause problems in the body and are excreted via urine [15,16].

Because of the above-mentioned characteristics of Mg and its alloys, they are thought to be a good choice for the

Corresponding author. E-mail: kashanian_s@yahoo.com

manufacturing of cardiovascular (*e.g.,* stent) and orthopedic (*e.g*., bone plate, pin, and screw) implants [8,17]. The only disadvantage of Mg is its high rate of corrosion in the solutions containing chlorine like body fluids [8,18].

Within the last years, various techniques such as applying degradable coatings have been used to improve the corrosion resistance and corrosion control of Mg and its alloys [8].

These coatings are applied to the surface using various techniques, *e.g*. electrospinning [19]. Electrospinning is known as a viable, simple, and economical technique to produce excellent, and continuous fibers in micro- and nano- meter dimensions [14,20,21].

In this method, a wide range of polymers can be electrolyzed using various solvents, including water, without the risk of solvent evaporation. The electrospinning technique is based on applying a high voltage between the needle tip and the metal collector to produce uniform fibers [22].

One of the first polymers synthesized in the early 1930s is PCL, which is also one of the most important biodegradable polymers with excellent biocompatibility, significant toughness, high fracture energy and good mechanical strength compared to the most of other biocompatible polymers [23]. PCL polymers are often used as biomaterials in biomedical applications such as tissue engineering, diffusion-controlled delivery systems, wound dressing and scaffolds [14,24].

Cur (phenolic derivative) is obtained from the rhizome of turmeric [25-27]. According to practitioners of traditional China and Indian medicine [25], Cur powder cures many diseases such as cough, Alzheimer, and cancer [28-30]. Besides these properties, it is also attractive because of its stability, availability, safety, and low cost [21], and its other properties are being anti-inflammatory, antimicrobial, potent antioxidant and anti-corrosion properties [31-34]. The controlled release of Cur has been reported by different researchers using several drug delivery systems such as nanoparticles and nanofibers [30].

SA has features such as biocompatibility, biodegradability, non-toxicity, hydrophilicity, and it also has a relatively low cost. It has been used in various forms to control corrosion of metals in corrosive environments but because of the high viscosity, solubility limits, and high internal hydrogen bonding, spinning of this polymer using the electrospinning technique is a big challenge [35,36]. For this reason, it must be combined with other non-toxic and non-ionic polymers such as polyvinyl alcohol (PVA). These polymers facilitate the electrospinning process by forming hydrogen bonds with SA.

From 2016 to 2019, different polymer coatings such as poly(lactide) (PLA)/hydroxyapatite (HA), poly(3-hydroxybutyric acid-co-3-hydrovaleric acid), PCL/HA/simvastatin, and polypropylene carbonate (PPY-carbonate) have been used respectively to control the corrosion of different alloys of Mg implants, and after different investigation periods, they succeeded in reducing the corrosion rate of implants in the body [23,37-39].

The aim of this study was to control the corrosion of Mg (alloy AZ31) implants using nanofiber coatings in SBF [40-43]. For this purpose, we used PCL polymeric coating in the presence of Cur using electrospinning technique in order to prevent infection and inflammation of the damaged tissue in the first days of implant placement through slow release over a week. The polymer coating and the drug mentioned were examined using various techniques in the seven-day period.

EXPERIMENTAL

Reagents and Materials

The polymers and drugs used in this study, *i.e.* PCL, SA, PVA and, Cur were purchased from Sigma Aldrich. In addition, the utilized solvents including dimethylformamide (DMF), dichloromethane (DCM) and acetone were purchased from Merck, Germany. The salts (NaCl, $NaHCO_3$, KCl, K_2HPO_4, $MgCl_2.6H_2O$, HCl(1M), $CaCl_2$, Na_2SO_4, Tris(hydroxymethyl)aminomethane (Tris)) used to prepare SBF were also purchased from Merck.

Instrumentation

The devices used in this study are: balance (Switzerland, mettle), heater/stirrer (MR 3002) (Heidolph) electrification device (Nano Ris), optical microscope (Euromex), ultrasonic bath (*Italy, Euronda),* oven **(**Vietnam, Memmert), UV-Vis spectrophotometer (8453) (Agilent), FT-IR spectropolarimeter (Japan, Jasco FTIR-4200), contact angle (Jikan Surface Nano-Engineering Company), scanning

electron microscopy (SEM) (TE-SCAN), 827 pH lab (Metrohm), and electrochemical impedance spectroscopy (EIS) (The Netherlands, Eco Chemie B. V.).

Preparation and Electrospinning of the Polymer Solution

To prepare one ml of 12.5 wt% PCL solution, 0.125 g of solid PCL was dissolved in one ml of DMF and DCM at a ratio of 2:1. To complete dissolution, the prepared solution was stirred for 4 h at 500 rpm (at room temperature). Then, to prepare PCL-Cur solution, 0.00125 and 0.02 g of Cur was added to the PCL solution to make 1 and 16 wt% of Cur [44], then the final solution was stirred for 1 h at 700 rpm.

In order to produce the desired nanofibers, electrospinning parameters such as voltage, distance and current flow rate should be optimized. Hence, after the preparation of the PCL and PCL-Cur solutions, the voltages of 16, 18, and 20 kV, flow rates of 1, and 0.7 ml h^{-1} and distances of 14, 16, 18, and 20 cm were investigated to produce nanofiber. Finally, according to the optical microscopic images of the different samples, we chose the values of 16 kV, 1 ml h^{-1}, and 16 cm as optimum values for voltage, flow rate and distance, respectively.

To make 1 ml of 3 wt% SA solution, 0.03 g of SA was added to 0.97 g of water. Then, it was placed on the stirrer at 750 rpm. Meanwhile, 0.1 g of PVA was dissolved in 0.9 g of deionized water, and it was stirred for 2 h. At the end of 2 h, the prepared solutions were added together with the ratio of 1:1. We electrolyzed SA-PVA solution at voltage, flow rate, and distance of 16 kV, 0.7 ml h^{-1} and 16 cm, respectively.

Characterization of Nanofibers

SEM, FT-IR, and CA were used to investigate the morphology and measure the diameter of different fibers, and also the structure and chemistry of PCL polymer in the presence of Cur and as well as to evaluate the hydrophobic change of PCL in the presence of Cur and SA-PVA [38,45].

To investigate the release of the drug from nanofibers and, choosing the optimized drug concentration, the release rate of the drug loaded within the nanofibers (with different concentrations) was examined using a spectrophotometer (426 nm) in phosphate-buffered saline (PBS) pH 7.4, at 37 °C [46].

Preparation of Mg Metal

Before coating the polymer on the metal, the following steps were taken to thoroughly clean and prepare the surface:

(I) metal cutting using saw at the dimension of 15 × 10 × 4 mm^3, (II) polishing of the metal surface using SiC paper with 400 and 2000 graits, (III) soaking metals in acetone for 10 min, (IV) putting up in the ultra-sonicate bath for 15 min, (V) soaking in distilled water for 10 min, (VI) drying the metal specimens by placing it in an oven at 60 °C for 40 min. After performing the above steps, the energy dispersive x-ray spectroscopy (EDX) was used to determine the AZ31 alloy and the percentage of the various elements in it.

Metal Corrosion Characterization

SEM analysis was done to investigate the morphology and surface degradation of uncoated and fiber-coated specimens after a seven-day immersion period.

Corrosion testing of different specimens was performed by potentiodynamic polarization and EIS. For both tests, a three-electrode system and SBF were deployed as electrolyte solutions. Mg samples of uncoated and with different coatings were used as working electrodes, Ag/AgCl in KCl solution as the reference electrode, and platinum as the auxiliary electrode. Before performing the test, the working electrodes (1 cm^2) were exposed to the SBF solution at 37 °C temperature to create a steady-state, for 30 min [14].

The degradability of different samples was explored through following the SBF pH changes [23]. For this purpose, the pH values for each sample was measured during a three-day immersion period at predetermined times. During this period, each sample was kept in a bottle containing 15 ml SBF at 37 °C.

One of the simplest and oldest ways to check metal corrosion is to measure weight loss. To perform this test, we measured the weight of the different samples after coating and drying the polymer on the Mg pieces (10 × 15 × 2 mm^3). Then, we immersed samples in the SBF for a week

(the buffer was changed every three days). At the end of the immersion period, the samples were removed from the buffer and were washed with distilled water then weighed after 48 h of drying [47].

RESULTS AND DISCUSSION

Nanofibers Related Analysis

Drug release. Figure 1a shows the release curves of 1 and 16% Cur. These curves have been plotted using the calibration diagram shown in Fig. 1b. As it can be seen from the release graphs, both concentrations have a burst release in the first 24 h. Nevertheless, the intensity of the burst release in the early 24 h for 1% Cur was higher. This type of release relates to drugs available at the nanofiber surface. After 24 h, the release of both concentrations continued with a mild slope which is attributed to the drug within the nanofiber structure. At the end of the seven days, the nanofibers contained 1%, and 16% Cur showed 96.97% and 74.59% of the release, respectively. The amounts of the initial loaded drug for 1 and 16% Cur were 3.52 and 5.86 µM, respectively. Due to the initial loaded values and their release percentages, at the end of the week, 3.38 and 4.37 µM were released from nanofibers containing 1% and 16% Cur, respectively (according to the amount of their absorption and the equation of the calibration plot).

Therefore, it can be said that the antibacterial property of 16% Cur nanofiber is higher. Finally, after making sure that a suitable release chart can be provided, we continued the experiment using 16% Cur nanofiber. On the other hand, the allowed dose of Cur is 10 µM [26] and the amount of drug released from the nanofibers produced is still less than the allowed dose in the body. Moreover, the excess amount of this drug in the body does not cause any problems and side effects [48,49].

Morphological Investigations

The results of the fiber-prepared SEM are indicated in Figs. 2a-c. As shown, all three cases of PCL, PCL-Cur, and SA-PVA possess uniform and continuous strands, and their average diameters were obtained 171.57, 179.60 and 157.06 nm, respectively. There is no significant difference between a and b SEM images and their diameters. This indicates the ineffectiveness of 16% Cur on the morphology

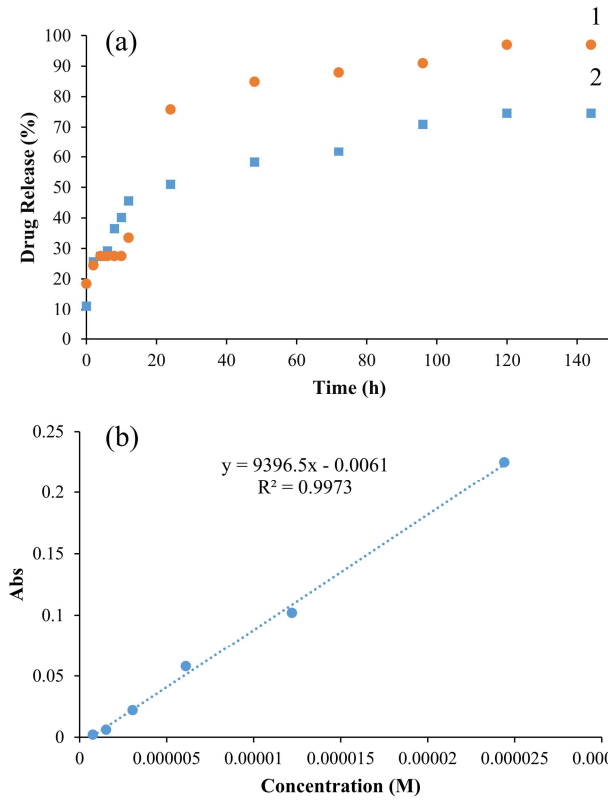

Fig. 1. (a) Curves of Cur release in PCL nanofibers. (1) Cur 1%. (2) Cur 16%. (b) Calibration release diagram of Cur.

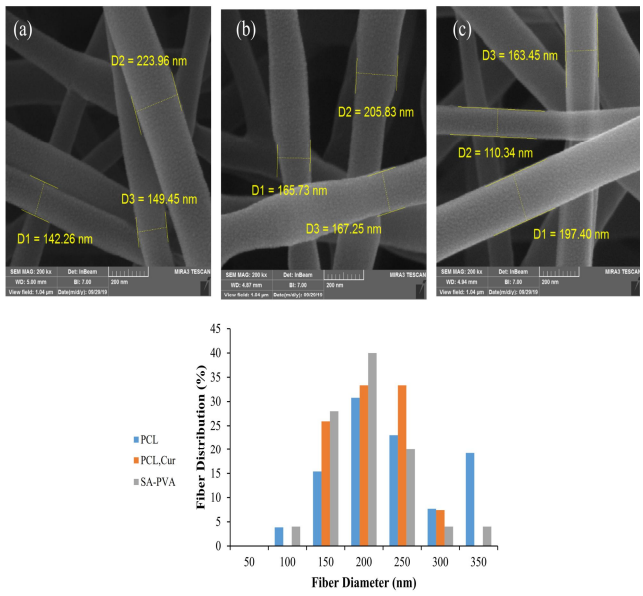

Fig. 2. (a-c) SEM images and histogram chart of prepared nanofibers (a) PCL fiber (b) PCL-Cur (c) SA-PVA.

and size of the PCL fiber diameter. SA-PVA also has nanometer-sized fibers, with a diameter of less than 200 nm.

In Figs. 3a-c we see the results of the CA test images. PCL is a hydrophobic substance, so the buffer penetrates harder into it. In this study, the amount of CA of PCL nanofibers was 146.6, which is consistent with the results of previous studies [14,30,50]. The amount of CA of this fiber decreased slightly in the presence of Cur and approached 135.2. It can be said that Cur has a positive effect on the better adhesion of the coating to the metal. The CA of the SA-PVA/PCL-Cur has further reduced. In this coating, we used SA-PVA as an undercoat and its CA value was equal to 126.5. Again, it could be said that reducing the CA value results in better fiber adhesion to the metal. This result gets us closer to the goal of SA usage. Of course, SA also has anti-corrosion properties in addition to its adhesion properties. Nevertheless, according to the results of other tests, we found out that although SA-PVA increases the adhesion of the coating, it is degraded earlier than PCL and Cur due to its hydrophilicity. Therefore, it can be said that it does not function well for corrosion control in these conditions.

The FTIR spectrum of electrolyzed PCL polymer demonstrates three clear peaks at 2900, 1700, and 1100 cm^{-1} wavelengths which belong to the functional groups asymmetric CH_2 stretching, -CO stretching in the ester carbonyl group, and C-O bonding, respectively [23,45]. Cur also has clear peaks at the wavelengths of 3408, 1627, 1583, and 1461 cm^{-1}, which belong to the O–H stretching vibration of the phenol group, carbonyl group C=O, vibrating tensile of C–C of the benzene ring, and benzene ring olefin bond, respectively [45]. The peaks of both substances are present in the spectrum of electrolyzed PCL-Cur, *i.e.* the peaks at the wavelengths of 3400, 2900, 1870, and 1600 cm^{-1}, which confirm the presence of Cur in PCL fiber and explain the change in PCL chemistry in the result of the existence of Cur (Fig. 4a).

Metal Related Analysis

In Fig. 4b and Table 1, the results of the EDX analysis related to the Mg metal AZ31 alloy are reported. The percentage of different elements such Mg, Al, Mn, Fe, and Zn confirms that the used alloy was type AZ31. The results

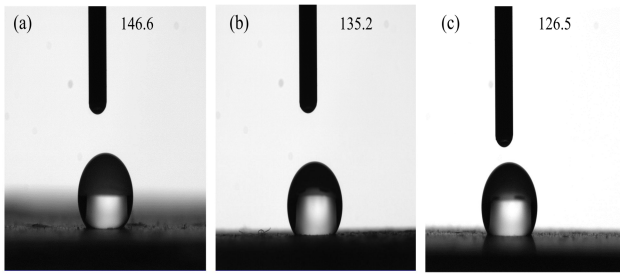

Fig. 3. (a-c) The result of contact angle of the different coating surfaces (a) PCL (b) PCL-Cur (c) SA-PVA/PCL-Cur.

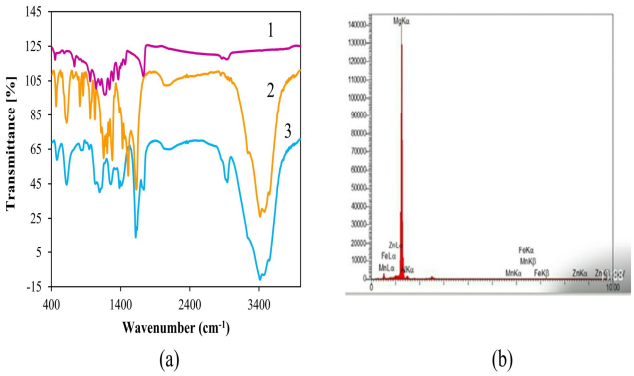

Fig. 4. (a) FTIR spectra of fibers (1) PCL (2) Cur (3) PCL-Cur. (b) EDX results of the AZ31 magnesium alloy surface.

Table 1. EDX Quantitative Results of the AZ31 Magnesium Alloy Surface

Elt	Mg	Al	Mn	Fe	Zn
W%	94.96	2.96	0.30	0.38	1.40

are in agreement with the results of the previous works [17,23,38,51].

Metal Corrosion Related Analysis

The SEM images of the bare sample and the coated samples before and after the immersion in SBF are shown in

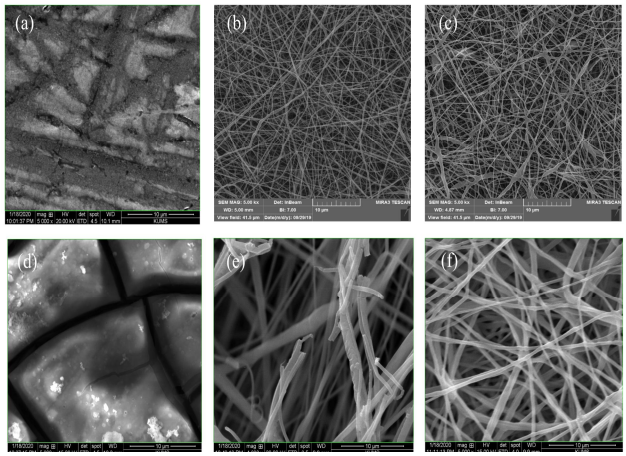

Fig. 5. The SEM images before immersion of the (a) bare sample, (b) PCL-coated sample, (c) PCL-Cur coated sample, and after immersion of the (d) bare sample, (e) PCL-coated sample, (f) PCL-Cur coated sample.

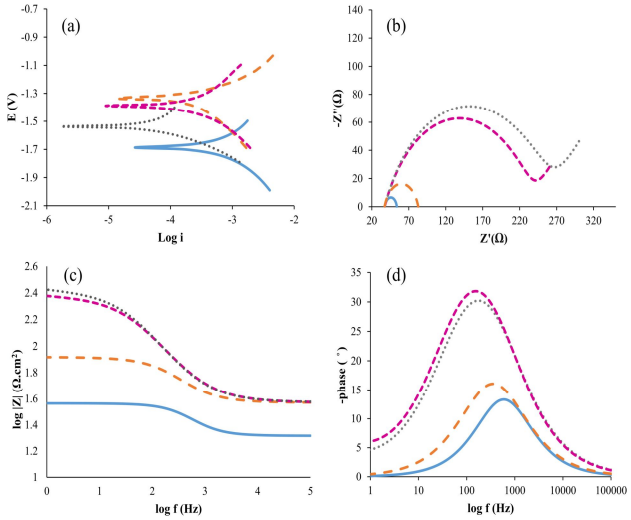

Fig. 6. (a) Potentiodynamic polarization curve of different samples in SBF (b) Nyquist, (c) bode and (d) phase angle of EIS analysis for different samples in the SBF at 37 °C. SA-PVA/PCL-Cur (Gray), PCL-Cur (violet), PCL (yellow), Bare (blue).

Fig. 5. In the bare sample images before immersion, only a few lines can be seen, which are related to Mg structure and the polishing step in the metal preparation process. To make the metal surface smoother, it is better to use higher grade paper. Images of the bare specimen after immersion show many cracks and holes on the metal surface. It can be said that the corrosion occurred mainly in the cavity type. In the image related to the PCL-coated sample we can see a smooth and uniform surface before immersion, but the rupture in some strands and the degradation of some parts of the PCL fibers after the seven-day immersion period are clearly seen in the SEM images. As indicated, the SEM images of the PCL-Cur-coated sample before and after immersion are not different. An important point is that there is no degradation or rupture in any parts of the nanofiber after immersion. According to the SEM pictures, it can be said that Cur addition to PCL nanofibers had a significant effect on the fiber strength. In the case of nanofibers covered with SA-PAV/PCL-Cur, the coating was completely removed from the surface due to the faster degradation of the SA before the end of the immersion period.

In this study, the polarization potential test was used to investigate the corrosion resistance of different surfaces (Fig. 6a). Using polarization diagram, we calculated the parameters of corrosion potential (E_{corr}), corrosion current density (I_{corr}), and finally, we obtained the corrosion rate (C_R; mm y^{-1}) and polarization resistance (R_P; kΩ cm^2) for different samples using the following Eqs. ((1), (2)) [23,52]:

$$C_R = \frac{3270 I_{corr} \times M}{V \times D} \quad (1)$$

$$R_p = \frac{b_a \times b_c}{2.3 I_{corr} (b_a + b_c)} \quad (2)$$

Where M, V, and D are the atomic mass, the number of metal exchanged electrons, and sheet density, respectively.

The values of the mentioned parameters as well as the anodic Tafel slopes (b_a) and the cathodic Tafel slopes (b_c) have been listed in Table 2 for different samples. As indicated in Table 2, the amount of corrosion current density decreases with increasing corrosion potential; As a result, the R_p and C_R increase and decrease, respectively. According to the plotted diagrams, it can be said that the amount of E_{corr} of bare Mg is lower than that of all coated samples. Among the coated samples, the PCL-coated sample had more E_{corr} compared to the other coated

Table 2. Electrochemical Parameters of Different Samples in SBF

Samples	E_{corr} (V)	I_{corr} (μA)	b_a	b_c	C_R (mm y^{-1})	R_p (kΩ cm^2)
Bare	-1.69	26.67	0.143	-0.17	0.59	1.25
PCL	-1.34	14.16	0.16	-0.22	0.31	2.82
PCL-Cur	-1.39	8.99	0.23	-0.15	0.20	4.41
SA-PVA/PCL-Cur	-1.54	1.73	0.13	-0.10	0.039	14.79

specimens. This is due to the higher hydrophobicity of monolayer PCL than the other two coatings. PCL-Cur and SA-PVA/PCL-Cur coatings are more hydrophilic due to the presence of Cur, PVA and SA, which reduces the E_{corr} values of these coatings. Between the PCL-Cur and SA-PVA/PCL-Cur coatings, the hydrophilic amount of the second coating is higher due to the presence of SA and PVA. In addition to Cur, and as a result, its E_{corr} is lower than that of the PCL-Cur coating.

To better investigate the corrosion behavior of the various samples in this study, EIS spectra were obtained in the open potential circuit (OCP). The results of the Nyquist plot, bode plot, and phase angle plot are given in Figs. 6b, c and d, respectively.

The Nyquist plot indicates the resistance to charge transfer and capacitance of the double electric layer between the electrode and the electrolyte solution. As seen in Fig. 6b, the coated samples have a higher impedance (-Z" and Z') than the bare sample. This means that samples coated with different nanofibers have insulation and resistance properties against corrosion. PCL-Cur-coated sample and sample coated with SA-PVA undercoat have the largest impedance; of course, the radius of the sample covered with SA-PVA undercoat is slightly larger, which is attributed to the use of two-layer nanofibers for this sample. As can be seen in Fig. 6b, the radius of the impedance spectra is related to two mentioned samples that are very different from the PCL-coated and the bare samples. The large impedance of the sample coated with PCL-Cur is attributed to hydrophobicity and insulation of PCL and Cur against buffer penetration, and as a result, their corrosion resistance [14]. To simulate the impedance spectra of different samples, we used the [R(Q[RW])] equivalent electrical circuit (EEC). Using [R(Q[RW])]'s EEC, we obtained a more fitting spectrum that had a smaller x^2. In this type of electrochemical study, two types of resistors can be examined: solution resistance (R_{sol}) and charge transfer resistance (R_c).

Due to the use of the same electrolyte solution for all samples, the R_{sol} was equal for all samples, and we only investigated Rc of different coatings. Accordingly, the charge R_c values for the bare sample, the samples coated with PCL and PCL-Cur nanofiber, and the sample with pre-layer of SA-PVA were 16, 45.7, 200, and 223 ohms, respectively. In fact, the R_c value of the sample with nanofibric coatings containing Cur was approximately 12 times higher than that of the bare sample and 4 times higher than that of the sample coated with the Cur-free nanofibers.

These results were also confirmed by the results of the bode plot. Figure 6c shows the bode plot for various samples mentioned. As it is known, the impedance module |Z| is drawn versus frequency in the bode spectrum and a larger |Z| in the lower frequency range indicates better corrosion resistance of the substrate [14]. As it could be seen the samples with SA-PVA pre-layer and covered with PCL-Cur have the largest modulus of impedances, and they have a significant difference with the bare and PCL-coated samples. The presence of dense and compact layers in the mentioned coatings plays an important role in the increasing of the impedance modulus.

To investigate the corrosion mechanism of the mentioned samples, the phase angle spectrum was investigated as a function of frequency (Fig. 6d). As shown in Fig. 6d, the coated and bare samples have different mechanisms. The phase angle of the coated specimens that have capacitive behavior relative to the frequency moves

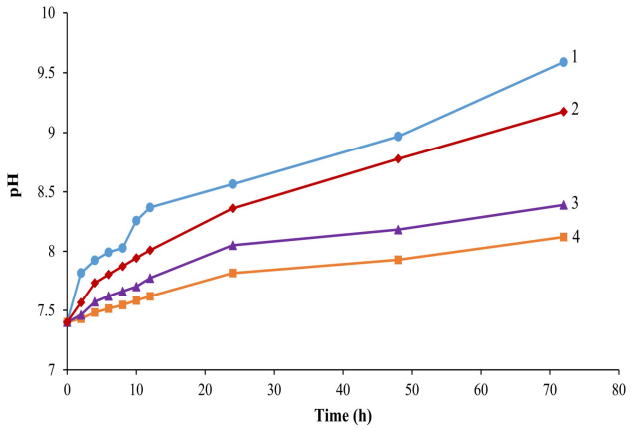

Fig. 7. pH value Change of different samples in SBF at different time intervals. (1) Bare (2) SA-PVA/PCL-Cur (3) PCL-Cur (4) PCL.

toward more negative frequencies. In fact, coated specimens are more insulating than bare specimens. The difference in the corrosion mechanism and being insulation of samples with SA-PVA pre-layer and covered with PCL-Cur compared to the bare sample is much greater than the difference in the corrosion mechanism of the sample covered with PCL compared to the bare sample.

Figure 7 shows the changes of SBF pH for the bare and coated samples. The pH value has increased for all samples which is due to the hydroxide ions production during the process of Mg degradation. The increase in pH value for the bare sample was the most significant compared to all coated samples. The pH value for the bare sample increased from 7.4 to 9.6 after three days. The results of the pH test also confirm the reduction in the corrosion rate of the metal by the coating application. As could be seen, the increase in pH value for the samples coated with PCL and the sample coated with SA-PVA undercoat is greater than the PCL-coated sample. In these coatings, Cur is a strong base (pK_a = 7.7-10.7) and SA is a weak base (pK_a = 3.7) and they increase the value of pH from the beginning of the pH measurement.

The percentages of weight loss of different samples are calculated, using Eq. (3), and reported in Table 3 [53,54]; the weight loss percentage ratio of each sample to bare ones is reported in Table 3 as well.

$$Weight\ loss\ (\%) = \frac{W_0 - W_t}{W_0} \times 100 \quad (3)$$

Where W_0 and W_t are the initial weight of the metal before immersion and secondary metal weight after immersion respectively.

Bare Mg had the highest percentage of weight loss in the SBF. This weight loss for the PCL-coated sample is half of the amount of the related bare sample. Whereas the weight loss percentage of the PCL-Cur-coated sample is one-fifth of the bare sample, which has significantly reduced compared to the bare and PCL-coated samples. For coated sample with SA-PVA as the undercoat, this value was half of the amount of related bare sample, and it can be said that it served almost the same function as the PCL-coated sample.

CONCLUSIONS

Biocompatible and biodegradable polymer coatings are used to control the corrosion rate of Mg implants. In this study, the coatings of PCL, PCL-Cur, and SA-PVA/PCL-Cur were produced using the electrospinning technique, with continuous and uniform strands and diameters in the

Table 3. The percentages of Weight Loss of Different Samples

Sample	Before immersion (g)	After immersion (g)	Weight difference (g)	Weight loss (%)
Bare	0.9582	0.9547	0.0035 (±0.0001)	0.37
PCL	0.8608	0.8593	0.0015 (±0.0001)	0.17
PCL-Cur	0.9190	0.9183	0.0007 (±0.0001)	0.07
SA-PVA/PCL-Cur	1.0405	1.0387	0.0016 (±0.0001)	0.15

nanoscale range. From the results of SEM, polarization, EIS and weight measurement tests, it was found out that the PCL-Cur polymer coatings had the best performance during the study period and no damage was done to the mentioned coating. Therefore, it can be said that Cur addition to the PCL, not only provides antibacterial properties, but also increases the strength of the fiber. The values of the weight loss results and R_p and C_R of the EIS test related to the PCL-Cur coating also confirm the positive effects of Cur addition and better performance of this coating compared to the PCL coating. In the case of SA-PVA/PCL-Cur cover, where SA-PVA was used as a pre-layer with anti-corrosion and more adhesion properties, it was destroyed more quickly than PCL because of its more hydrophilicity, and we did not get the desired result in the mentioned conditions. In general, it can be said that the corrosion rate of Mg implants decreased significantly by applying PCL-Cur polymeric coating compared to the bare and/or other coating samples.

ACKNOWLEDGEMENTS

The authors gratefully acknowledge the financial support from Razi University and the Nano Drug Delivery Research Center of Kermanshah University of Medical Sciences.

REFERENCES

[1] J.L. Gilbert, Corrosion 73 (2017) 1478.
[2] D. Sivaraj, K. Vijayalakshmi, J. Alloys Compd. 777 (2019) 1340.
[3] S. Jafari, S.E. Harandi, R.S. Raman, Jom. 67 (2015) 143.
[4] Y.-K. Kim, K.-B. Lee, S.-Y. Kim, K. Bode, Y.-S. Jang, T.-Y. Kwon, M.H. Jeon, M.H. Lee, Sci. Technol. Adv. Mater. 19 (2018) 324.
[5] W. Liu, Z. Yan, X. Ma, T. Geng, H. Wu, Z. Li, Materials 11 (2018) 396.
[6] K. Munir, J. Lin, C. Wen, P.F. Wright, Y. Li, Acta Biomater. 102 (2020) 493.
[7] L. Córdoba, M. Montemor, T. Coradin, Corros. Sci. 104 (2016) 152.
[8] T. Hanas, T.S. Kumar, Mater. Today: Proc. 4 (2017) 6697.
[9] D. Zander, N.A. Zumdick, Corros. Sci. 93 (2015) 222.
[10] Y. Ogawa, D. Ando, Y. Sutou, J. Koike, Science 353 (2016) 368.
[11] S. Gaur, R.S. Raman, A.S. Khanna, Mater. Sci. Eng. C 42 (2014) 91.
[12] S. Jafari, R.S. Raman, C.H. Davies, Eng. Fract. Mech. 137 (2015) 2.
[13] T.S. Narayanan, I.S. Park, M.H. Lee, Prog. Mater. Sci. 60 (2014) 1.
[14] J. Kim, H.M. Mousa, C.H. Park, C.S. Kim, Appl. Surf. Sci. 396 (2017) 249.
[15] S. Jafari, R.S. Raman, Mater. Sci. Eng. C 78 (2017) 278.
[16] P. Chakraborty Banerjee, S. Al-Saadi, L. Choudhary, S.E. Harandi, R. Singh, Materials 12 (2019) 136.
[17] G.K. Soujanya, T. Hanas, V.Y. Chakrapani, B.R. Sunil, T.S. Kumar, Procedia Mate. Sci. 5 (2014) 817.
[18] J. Ma, M. Thompson, N. Zhao, D. Zhu, J. Orthop. Translat 2 (2014) 118.
[19] A. Groysman, Springer Science & Business Media., 2009.
[20] M.M. Mahmud, S. Zaman, A. Perveen, R.A. Jahan, M. F. Islam, M.T. Arafat, J. Drug Deliv. Sci. Technol 55 (2020) 101386.
[21] R. Leidy, Q.-C.M. Ximena, Trends Food Sci. Technol. 85 (2019) 92.
[22] A.I. Rezk, H.M. Mousa, J. Lee, C.H. Park, C.S. Kim, J. Coat. Technol. Res. 16 (2019) 477.
[23] P. Karuppuswamy, J.R. Venugopal, B. Navaneethan, A.L. Laiva, S. Ramakrishna, Mater. Lett. 141 (2015) 180.
[24] A. Blanco-Padilla, A. López-Rubio, G. Loarca-Pina, L.G. Gómez-Mascaraque, S. Mendoza, LWT-Food Sci. Technol. 63 (2015) 1137.
[25] P.-A. Mouthuy, M.S. Škoc, A.Č. Gašparović, L. Milković, A.J. Carr, N. Žarković, Int. J. Nanomedicine. 12 (2017) 3977.
[26] X.-Z. Sun, G.R. Williams, X.-X. Hou, L.-M. Zhu, Carbohydrate Polymers 94 (2013) 147.
[27] F. Attari, M. Zahmatkesh, H. Aligholi, S.E. Mehr, M. Sharifzadeh, A. Gorji, T. Mokhtari, M. Khaksarian, G.

Hassanzadeh, DARU J. Pharm. Sci. 23 (2015) 33.
[28] M. Ranjbar-Mohammadi, S.H. Bahrami, Int. J. Biol. Macromol. 84 (2016) 448.
[29] T. Elakkiya, G. Malarvizhi, S. Rajiv, T.S. Natarajan, Polym. Int. 63 (2014) 100.
[30] A. Fouda, K. Elattar, J. Mater. Eng. Perform. 21 (2012) 2354.
[31] V. Johnsirani, J. Sathiyabama, S. Rajendran, R. Nagalakshmi, Chem. Sci. Trans. 2 (2013) S123.
[32] A.S. Yaroa, K.F. Talib, Iraqi J. Chem. Pet. Eng. 15 (2014) 9.
[33] B. Vigani, S. Rossi, G. Milanesi, M.C. Bonferoni, G. Sandri, G. Bruni, F. Ferrari, Nanomaterials 8 (2018) 971.
[34] K.Y. Lee, L. Jeong, Y.O. Kang, S.J. Lee, W.H. Park, Adv. Drug Deliv. Rev. 61 (2009) 1020.
[35] A. Abdal-Hay, A. Hasan, M.-H. Lee, A.S. Hamdy, K.A. Khalil, Mater. Sci. Eng. C 58 (2016) 1232.
[36] J. Castro, K.G. Krishnan, S. Jamaludeen, P. Venkataragavan, S. Gnanavel, J. Bio- Tribo-Corros. 3 (2017) 52.
[37] Z. Zhao, L. Zhao, X. Shi, J. Liu, Y. Wang, W. Xu, H. Sun, Z. Fu, B. Liu, S. Hua, Proc. Estonian Acad. Sci. 68 (2019) 13.
[38] Z. Panahi, E. Tamjid, M. Rezaei, Surf. Coat. Technol. 386 (2020) 125461.
[39] M. Rahimi, R.M. Aghdam, M.H. Sohi, A.H. Rezayan, M. Ettelaei, Surf. Coat. Technol. 405 (2021) 126627.
[40] H.R. Bakhsheshi-Rad, M. Akbari, A.F. Ismail, M. Aziz, Z. Hadisi, E. Pagan, M. Daroonparvar, X. Chen, Surf. Coat. Technol. 377 (2019) 124898.
[41] G. Perumal, B. Ramasamy, M. Doble, Colloids Surf. B 172 (2018) 690.
[42] S.M. Saeed, H. Mirzadeh, M. Zandi, J. Barzin, Prog. Biomater. 6 (2017) 39.
[43] M. Roshandel, R. Sotudeh-Gharebagh, S. Mirzakhanlouei, R. Hajiaghaee, R. Ghaffarzadegan, J. Chem. Pet. Eng. 52 (2018) 181.
[44] R. Ravikumar, M. Ganesh, V. Senthil, Y.V. Ramesh, S.L. Jakki, E.Y. Choi, J. Drug Deliv. Sci. Technol. 44 (2018) 342.
[45] A.S.K. Kiran, A. Kizhakeyil, R. Ramalingam, N.K. Verma, R. Lakshminarayanan, T.S. Kumar, M. Doble, S. Ramakrishna, Ceram. Int. 45 (2019) 18710.
[46] L. Basir, S. Kalhori, A.Z. Javid, M.K. Masjedi, J. Natl. Med. Assoc. 110 (2018) 486.
[47] S. Zorofchian Moghadamtousi, H. Abdul Kadir, P. Hassandarvish, H. Tajik, S. Abubakar, K. Zandi, Biomed. Res. Int. (2014).
[48] V.Y. Chakrapani, A. Gnanamani, V. Giridev, M. Madhusoothanan, G. Sekaran, J. Appl. Polym. Sci. 125 (2012) 3221.
[49] A. Srinivasan, P. Ranjani, N. Rajendran, Electrochim. Acta 88 (2013) 310.
[50] M. Cui, C. Xu, Y. Shen, H. Tian, H. Feng, J. Li, Thin Solid Films 657 (2018) 88.
[51] A.W. Nafi, A. Afifi, N.I.Z. Abidin, A. Aziz, N. Hidayah, K. Kalantari, Sains Malays. 47 (2018) 169.
[52] A. Suryavanshi, K. Khanna, K. Sindhu, J. Bellare, R. Srivastava, Biomed. Mater. 12 (2017) 055011.